ELSEVIER

Physica B 244 (1998) 1–8

PHYSICA B

Superfluid and normal fluid density in high-T_c superconductors

D.B. Tanner[a,*], H.L. Liu[a], M.A. Quijada[a], A.M. Zibold[a], H. Berger[b], R.J. Kelley[c], M. Onellion[c], F.C. Chou[d], D.C. Johnston[d], J.P. Rice[e], D.M. Ginsberg[e], J.T. Markert[f]

[a] *Department of Physics, University of Florida, Gainesville, FL 32611-8440, USA*
[b] *Institut de Physique Appliquée, EPF de Lausanne, CH 1015 Lausanne, Switzerland*
[c] *Department of Physics, University of Wisconsin, Madison, WI 53706, USA*
[d] *Ames Laboratory and Department of Physics and Astronomy, Iowa State University, Ames, IA 50011, USA*
[e] *Department of Physics, University of Illinois, Urbana, IL 61801, USA*
[f] *Department of Physics, University of Texas, Austin, TX 78712, USA*

Abstract

The electronic properties of the cuprate superconductors have been studied by measuring the reflectance over the frequency range from the far-infrared to the near-ultraviolet (roughly, 10 meV–5 eV). There is an interesting behavior in both the normal state and the superconducting state. In the normal state, there is the well-known non-Drude distribution of the doping-induced spectral weight. In the superconducting state, the spectral weight of the superconducting condensate correlates with T_c in a variety of materials. Remarkably, in optimally doped superconductors, only about 20% of the doping-induced carriers joins the superfluid; the rest of the spectral weight remains at finite frequencies.

Keywords: Superconductivity; Optical properties; High-temperature superconductors; Far-infrared spectroscopy

1. Introduction

In this paper, we study the distribution of doping-induced and superfluid spectral weight (or oscillator strength) in cuprate materials. Undoped cuprates are generally described as "charge-transfer" insulators [1, 2] which become high-T_c superconductors when doped appropriately. The doping process introduces mobile carriers and is accompanied by a growth in low-energy spectral weight and a corresponding decrease in the oscillator strength of the charge-transfer band [3–6].

The spectral weight may be estimated by means of optical absorption through the partial sum rule on the conductivity [7]

$$\frac{m}{m^*} N_{\mathrm{eff}}(\omega) = \frac{2mV_{\mathrm{cell}}}{\pi e^2} \int_0^{\omega_c} \sigma_1(\omega')\, \mathrm{d}\omega', \tag{1}$$

where m^* is the effective mass, V_{cell} the unit-cell volume, and $\sigma_1(\omega)$ is the real part of the optical conductivity. The integral is over the range between zero and the onset of the charge-transfer excitation, $\sim 12\,000\ \mathrm{cm}^{-1}$. In what follows, the

*Corresponding author. Fax: +1 352 392 3591; e-mail: tanner@phys.ufl.edu.

0921-4526/98/$19.00
PII S0921-4526(97)00453-5

effective mass m^* is taken to be the free-electron mass m.

In the superconducting state, some of this spectral weight occurs in the zero-frequency delta-function response of the superfluid condensate, which is responsible for the infinite DC conductivity. From the sum rule, the area in the delta function is removed from the finite-frequency conductivity [8]. There are several ways to estimate this area. First, the difference in $N_{\rm eff}(\omega)$ computed in the normal and the superconducting states represents the area in the delta function, because the optical data in the superconducting state begin at low but finite frequencies and thus do not include the delta function.

Second, the weight of the delta function is related to the London penetration depth $\lambda_{\rm L}$ through

$$\frac{c^2}{\lambda_{\rm L}^2} = \frac{4\pi N_{\rm s} e^2}{m V_{\rm cell}}, \tag{2}$$

where $n_{\rm s} = N_{\rm s}/V_{\rm cell}$ is the superfluid density. Eq. (2) is a direct result of the Kramers–Kronig relation between the real and imaginary parts of the optical conductivity. The imaginary part, $\sigma_2(\omega)$, gives a frequency-dependent $\lambda_{\rm L}(\omega)$ via $c^2/\lambda_L^2 = 4\pi\omega\sigma_2(\omega)$. If one calculates $\lambda_{\rm L}(\omega)$ at low temperatures, one finds a reasonably flat curve whose zero-frequency value is the London length [9, 10]. This value can be used to estimate the superfluid density.

An equivalent way to obtain the superfluid density is to plot the real part of the dielectric function, $\varepsilon_1(\omega)$ versus $1/\omega^2$ [11]. From Kramers–Kronig, a zero-frequency delta function in $\sigma_1(\omega)$ at $\omega = 0$ gives a $1/\omega^2$ form to $\varepsilon_1(\omega)$

$$\varepsilon_1(\omega) = \varepsilon_\infty - \frac{\omega_{\rm ps}^2}{\omega^2}, \tag{3}$$

where $\omega_{\rm ps} = \sqrt{4\pi n_{\rm s} e^2/m^*}$ is the superfluid plasma frequency. This plot emphasizes the low-frequency behavior, which should be the most London like. The slope of the linear portion gives $\omega_{\rm ps}^2$, from which the superfluid density can be calculated, assuming $m^* = m$.

A third way to find this quantity is to make a fit of the reflectance to a sum of a narrow Drude function and Lorentzian oscillators. The narrow Drude function represents the zero-frequency delta function response of the superconductor.

There has been considerable interest in measuring the superfluid density, because it is of intrinsic interest by itself and because there has been shown to be a correlation between the number of carriers and the transition temperature [12]. Typically, the superfluid density is determined by a penetration-depth experiment, and calculated using Eq. (2). The principal result is that as the superfluid density increases so does the transition temperature, up to an "optimal-doping" level, when $T_{\rm c}$ is a maximum. Further doping drives the materials into the "overdoped" regime.

In the rest of this paper, then, we consider these optical measures of doping level, carrier density, and superfluid density. As an example, we show recent data for $Bi_{1.57}Pb_{0.43}Sr_2CaCu_2O_8$. We will also compare results for a variety of superconducting cuprates near optimal doping.

2. Experimental

Measurements were made on single crystals of cuprate superconductors grown using standard flux-growth techniques [13–17]. Typical crystal size was $2 \times 3 \times 0.2\,{\rm mm}^3$, with the *ab*-plane being the largest face. The infrared techniques [18] have been described previously. For the $Bi_{1.57}Pb_{0.43}Sr_2CaCu_2O_8$ crystal we covered 50–32 000 $\rm cm^{-1}$ at temperatures between 10 and 300 K using two spectrometers in conjunction with a flow cryostat for sample cooling. Most other materials were studied as a function of temperature from a low-frequency limit which varied from 30–150 $\rm cm^{-1}$, depending on sample size, to a maximum of 4000–5000 $\rm cm^{-1}$, with 300 K data up to 40 000 $\rm cm^{-1}$. That the temperature dependence was measured to high frequencies for the $Bi_{1.57}Pb_{0.43}Sr_2CaCu_2O_8$ sample makes it very useful for the study of the doping-induced spectral weight, although, as we shall see, there is not a lot of high-energy temperature dependence.

Most superconducting cuprates are orthorhombic; consequently, polarized studies of untwinned crystals are the most revealing and accurate. We have measured untwinned crystals of $YBa_2Cu_3O_7$, $Bi_2Sr_2CaCu_2O_8$, and $Bi_{1.57}Pb_{0.43}Sr_2CaCu_2O_8$. Our $Tl_2Ba_2CaCu_2O_8$ crystal had no measurable

anisotropy. We also measured twinned $YBa_2Cu_3O_7$ and La_2CuO_{4+x}.

3. Results: Reflectivity and conductivity

The *ab*-plane reflectance of $Bi_{1.57}Pb_{0.43}Sr_2CaCu_2O_8$ is shown in Fig. 1 at two temperatures: 10 K (upper panel) and 100 K (lower panel). The reflectance declines in an almost linear way to a plasma minimum around 10 000 cm^{-1}. Weak and temperature-independent bands occur at higher frequencies, with the charge-transfer band of the parent compound centered near 16 000 cm^{-1} (2 eV) but extending down to below the plasma minimum.

The superconducting transition has very little effect on the reflectance; the most evident feature is an increase at the lowest frequencies and a reversed-S shape below 1000 cm^{-1}. This region is shown in more detail in the insets to the figure. The sharp feature at 650 cm^{-1} is a phonon.

We performed a Kramers–Kronig analysis of the reflectance to estimate the phase shift on reflectance. From these quantities, reflectance and phase, any of the optical "constants" may be computed. We used conventional extrapolation schemes. At high frequencies data in the literature [19] were used, followed by a power-law (ω^{-4}) extrapolation. At low frequencies we fit the data to a Drude–Lorentz model, calculated the reflectance from the fit, and used this calculation as the low-frequency extension.

The optical conductivity in the infrared is shown in Fig. 2. The behavior is typical of cuprate superconductors: The low-frequency, normal-state conductivity is dominated by free-carrier (Drude) behavior. The zero-frequency peak in the conductivity grows and narrows with decreasing temperature.

This temperature-dependent part blends smoothly above about 500 cm^{-1} into a broad, slowly falling family of curves. At high frequencies, the conductivity is nearly temperature-independent.

Below T_c, the zero-frequency peak goes away, but there is no gap as occurs in the classic superconductors. [20, 21] Indeed, there is even a minimum in $\sigma_1(\omega)$ around 500 cm^{-1}, with a rising conductivity as $\omega \to 0$.

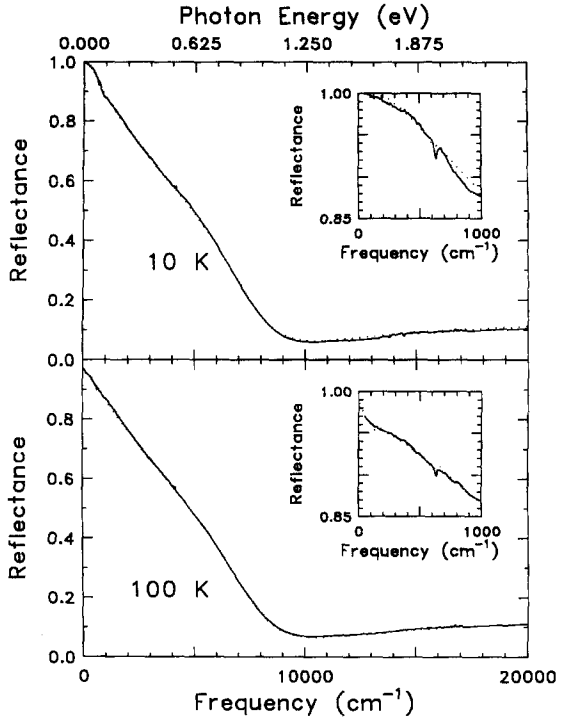

Fig. 1. Far-infrared reflectance of a $Bi_{1.57}Pb_{0.43}Sr_2CaCu_2O_8$ crystal at two temperatures. The insets show the low-frequency behavior.

4. Oscillator strength and carrier density

Inspection of Fig. 2 reveals that the spectral weight in the normal state is evidently conserved. As temperature is reduced, the increase in area at low frequencies is compensated by a decrease in area at high frequencies. However, below T_c, there is clearly a loss of area, which must be coming mostly from the free-carrier-like peak at $\omega \to 0$.

To make this discussion quantitative, we show in Fig. 3 the results of evaluating Eq. (1) for our data. Here we show $N_{eff}(\omega)$ on a per copper basis ($V_{cell} \approx 113$ Å^3). Two families of curves are seen, with only small differences within them. Above T_c, $N_{eff}(\omega)$ rises quickly and then begins to level off. We take as the carrier number the value of $N_{eff}(\omega)$ at

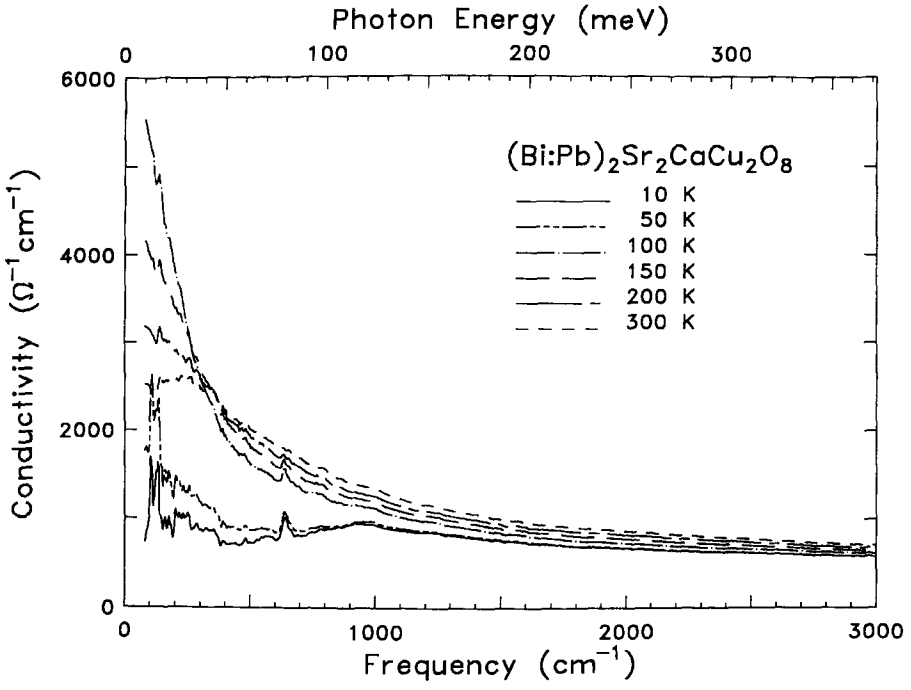

Fig. 2. Optical conductivity $\sigma_1(\omega)$ at six temperatures.

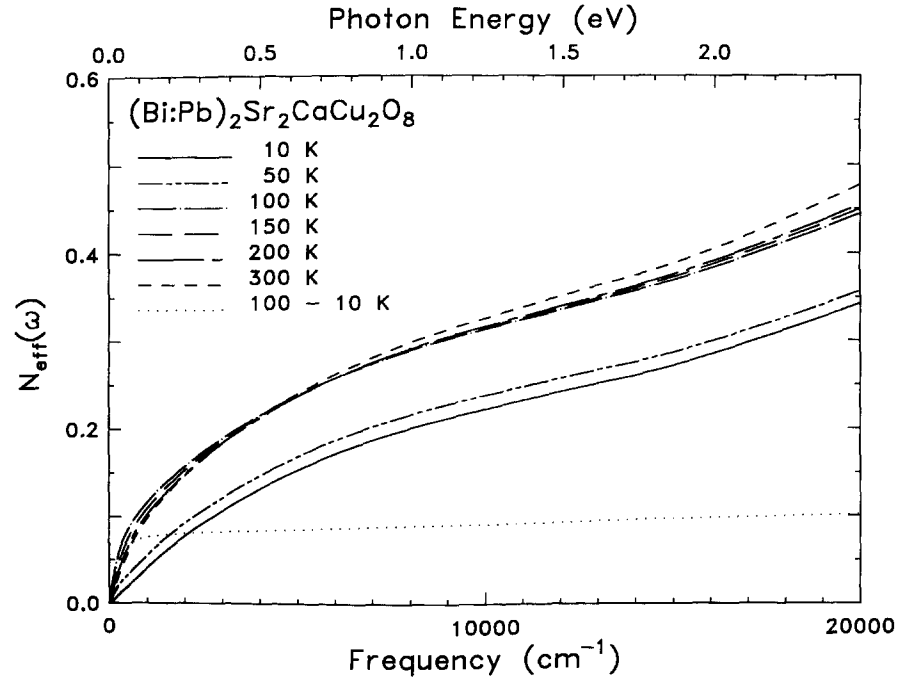

Fig. 3. The effective number of carriers in $Bi_{1.57}Pb_{0.43}Sr_2CaCu_2O_8$ participating in transitions less than ω for six temperatures. The difference between the 100 and 10 K results, which represents the spectral weight of the superfluid, is also shown.

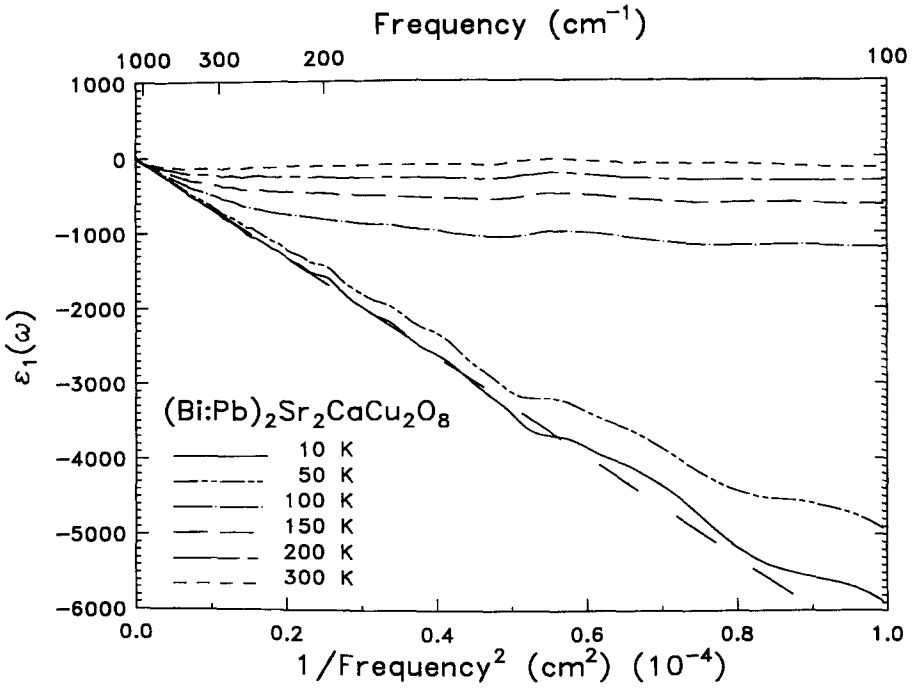

Fig. 4. $\varepsilon_1(\omega)$ versus $1/\omega^2$ at six temperatures. A fit of a straight line to the 10 K data is also shown.

12 000 cm^{-1}, just before the influence of the charge-transfer band begins to dominate the result, and get $N_{\text{eff}} \approx 0.36$ per copper in the normal state.

The superconducting-state curve rises more slowly, on account of the missing low-frequency spectral weight. The dotted line is the difference between 100 and 10 K. It is nearly horizontal, implying that the missing area is at the origin. Its value in the 2000–20 000 cm^{-1} region gives $N_s \approx 0.085$ per copper. Thus, only about a quarter to a fifth of the total doping-induced spectral weight appears in the delta function.

Our second method to estimate the weight of the delta function is to look at its influence on the real part of the dielectric function. A plot of $\varepsilon_1(\omega)$ versus $1/\omega^2$ is shown in Fig. 4. At high temperatures the low-frequency behavior (at the right of the figure) is approximately a constant, consistent with Drude behavior. Below T_c, however, the superfluid response dominates. The slope (dashed line) corresponds to $N_s \approx 0.085$ per copper.

Finally, we made a fit to a model which includes a narrow Drude peak at zero frequency, and used the oscillator strength of this narrow peak to estimate the superfluid density. The fit also gives the total oscillator strength below the charge-transfer gap and, in addition gives a number for the free carrier (Drude) density N_D in the normal state. The dotted lines in Fig. 1 are the results of such a fit. (The dotted lines are close enough to the data that they cannot be seen over much of the plotted range.) The 100 K data were fitted with four oscillators for the electronic bands in the region shown: a Drude at zero frequency and Lorentzian oscillators at $\sim$ 800, 5000, and 18 000 cm^{-1}. Two additional weak oscillators were used to fit the phonons. At 10 K in the superconducting state, most of the Drude oscillator strength has collapsed into the delta function at the origin, but about 5% of it remains in a normal-fluid component.

All three of the above methods give consistent results for the various contributions to the low-energy spectral weight for a variety of materials.

Table 1
Effective number of carriers per copper in a variety of cuprate materials. N_{eff} is the total doping-induced carrier density, N_s the number of superfluid carriers, and N_D the number of Drude carriers. Note that the number of coppers in $YBa_2Cu_3O_7$ was taken as 2 with polarization (Pol.) along the *a*-axis and as 3 for polarization along the *b*-axis

Material	T_c (K)	Pol.	N_{eff} /Cu	N_s /Cu	N_D /Cu	N_s/N_{eff} %	N_s/N_D %
La_2CuO_{4+x}[a]	40	*ab*	0.15	0.028	0.035	19	80
$Bi_{1.57}Pb_{0.43}Sr_2CaCu_2O_8$[b]	79	*ab*	0.37	0.085	0.097	23	87
$Bi_2Sr_2CaCu_2O_8$[c]	85	*a*	0.44	0.100	0.105	23	95
$Bi_2Sr_2CaCu_2O_8$[c]	85	*b*	0.48	0.090	0.096	19	94
$YBa_2Cu_3O_7$[d]	91	*a*	0.44	0.096	0.104	22	92
$YBa_2Cu_3O_7$[d]	91	*b*	0.59	0.125	0.16	21	78
$YBa_2Cu_3O_7$[e]	92	*ab*	0.44	0.082	0.093	19	88
$Tl_2Ba_2CaCu_2O_8$[b]	110	*ab*	0.54	0.115	0.13	21	88
Typical uncertainties	2		± 0.03	± 0.01	± 0.01	± 1%	± 4%

The sources of the crystals were:
[a]Ames laboratory;
[b]EFP de Lausanne;
[c]University of Wisconsin;
[d]University of illinois;
[e]University of Texas.

Results for several – all near optimum doping – are summarized in Table 1. This table shows the effective number of carriers *per copper* in (1) the low-energy region below the charge-transfer gap, (2) the superconducting condensate, and (3) the Drude or free-carrier part (from a two-component analysis). N_s is also shown as a fraction of N_{eff} and N_D.

There are four interesting features to these data: (1) There is a correlation between the number of carriers and the transition temperature [12]. This correlation holds whether one considers the number of carriers in the superfluid or the total number of carriers. (2) In untwinned $YBa_2Cu_3O_7$ we have included the chains in the count of the number of copper layers per unit cell when polarization is along *b* but not when along *a* or along *ab* in the twinned crystal. Even so, the number of carriers per copper *and* the number of carriers in the superfluid per copper are both larger for polarization along *b* than along *a*, in accord with the analysis that shows that the chain bands are closely involved with the superconductivity [9]. (3) In all materials, about 20–25% of the total doping-induced charge joins the superfluid; about 75–80% remains at finite frequencies. (4) If a two-component picture is adopted, then nearly 90% of the free-carrier spectral weight condenses.

5. Discussion

A key issue is the question – raised long ago in the context of the non-Drude behavior of the conductivity – of one or two components to the optical conductivity [22–24]. Is there a second component, i.e., a second type of charge carrier (generally called the "mid-infrared" carriers)? Or, is there only a single component with extremely unusual carrier damping/interactions?

The data gathered so far do not resolve this issue. In the two-component picture, a clean limit, weak coupling point of view, all of the free-carrier oscillator strength in the normal state is expected to condense into the zero-frequency delta function of the superfluid. This is approximately what happens, according to Table 1. However, if the second component is viewed as independent of the first, one expects no simple relation of the oscillator strengths of the two components. This is refuted by Table 1, where all the data give about a 4 : 1 ratio of mid-infrared to free-carrier spectral weight. If

there are two somewhat independent types of carriers introduced by doping, free carriers and bound carriers (perhaps on account of phase separation [25] or localization), it is not easy to understand why the ratio of densities of these components is the same in a variety of materials, especially when the individual densities vary by large amounts.

In the one-component picture, the non-Drude behavior comes from a strong frequency dependence to the quasiparticle damping. This picture was first presented in the context of the marginal Fermi liquid [26] and nested Fermi liquid pictures [27, 28] but it also occurs in the *d*-wave theories of the superconductivity [29, 30]. It is qualitatively consistent with the data for optimally doped $YBa_2Cu_3O_7$ [31] and $Bi_2Sr_2CaCu_2O_8$ [32] but not for underdoped $La_{2-x}Sr_xCuO_4$ [4] or for La_2CuO_{4+x} [33].

The one-component picture has a difficult task to account for the small value of the superfluid spectral weight. Because these materials are in the clean limit, the only way that the carriers can absorb light is through a process in which the emission of some excitation occurs [34–37]. The finite-frequency optical conductivity is related to the energy spectrum of these excitations. The oscillator strength in this Holstein sideband is a measure of the interaction strength between the carriers and the excitation, λ. The data in Table 1 imply $\lambda \approx 4$. This very-strong-coupling value is not consistent with the value 0.3 infrared from the temperature or frequency dependence of the quasiparticle damping [11, 32, 38].

In conclusion, neither of these opposing pictures is really supported by the data presented here. Either can be used to explain certain features of the data, but both run into difficulty with other details.

Acknowledgements

This research has been supported by NSF Grant DMR-9403894 at Florida, by NSF Grant DMR-89 11 332 at Wisconsin, by NSF Grant DMR-9 120 000 through the Science and Technology Center for Superconductivity at Illinois, and by NSF Grant DMR-9 705 414 at Texas. Ames Laboratory is operated for the US Department of Energy by Iowa State University under contract No. W-7405-ENG-82.

References

[1] J. Zaanen, G.A. Sawatzky, J.W. Allen, Phys. Rev. Lett. 55 (1985) 418.
[2] C.M. Varma, S. Schmitt-Rink, E. Abrahams Solid State Commun. 62 (1987) 681.
[3] S.L. Cooper, G.A. Thomas, J. Orenstein, D.H. Rapkine, A.J. Millis, S.-W. Cheong, A.S. Cooper, Z. Fisk, Phys. Rev. B 41 (1990) 11 605.
[4] S. Uchida, T. Ido, H. Takagi, T. Arima, Y. Tokura, S. Tajima, Phys. Rev. B 43 (1991) 7942.
[5] M.B.J. Meinders, H. Eskes, G.A. Sawatzky, Phys. Rev. B 48 (1993) 3916.
[6] H. Eskes, A.M. Oles, M.B.J. Meinders, W. Stephan, Phys. Rev. B 50 (1994) 17 980.
[7] Frederick Wooten, Optical Properties of Solids, Academic Press, New York, 1972.
[8] R.A. Ferrell, R.E. Glover, Phys. Rev. 109 (1958) 1398.
[9] D.N. Basov, R. Liang, D.A. Bonn, W.N. Hardy, B. Dabrowski, M. Quijada, D.B. Tanner, J.P. Rice, D.M. Ginsberg, T. Timusk, Phys. Rev. Lett. 74 (1995) 598.
[10] D.B. Tanner, M.A. Quijada, D.N. Basov, T. Timusk, R.J. Kelley, M. Onellion, J.P. Rice, D.M. Ginsberg, B. Dabrowski, S.-W. Cheong, F.C. Chou, D.C. Johnston, Ferroelectrics 177 (1996) 83.
[11] K. Kamarás, S.L. Herr, C.D. Porter, N. Tache, D.B. Tanner, S. Etemad, T. Venkatesan, E. Chase, A. Inam, X.D. Wu, M.S. Hegde, B. Dutta, Phys. Rev. Lett. 64 (1990) 84.
[12] Y.J. Uemura, L.P. Le, G.M. Luke, B.J. Sternlieb, W.D. Wu, J.H. Brewer, T.M. Riseman, C.L. Seaman, M.B. Maple, M. Ishikawa, D.G. Hinks, J.D. Jorgensen, G. Saito, H. Yamochi, Phys. Rev. Lett. 66 (1991) 2665.
[13] J.P. Rice, B.G. Pazol, D.M. Ginsberg, T.J. Moran, M.B. Weissman, J. Low Temp. Phys. 72 (1988) 345.
[14] P.D. Han, D.A. Payne, J. Crystal Growth 104 (1990) 201.
[15] D.B. Mitzi, L.W. Lombardo, A. Kapitulunik, S.S. Laderman, R.D. Jacowitz, Phys. Rev. B 41 (1990) 6564.
[16] F.C. Chou, J.H. Cho, D.C. Johnston, Physica C 197 (1992) 303.
[17] Allen M. Hermann, J.V. Yakhmi (Eds.), in: Thallium-Based High-Temperature Superconductors, Marcel Dekker, New York.
[18] F. Gao, D.B. Romero, D.B. Tanner, J. Talvacchio, M.G. Forrester, Phys. Rev. B 47 (1993) 1036.
[19] I. Terasaki, S. Tajima, H. Eisaki, H. Takagi, K. Uchinokura, S. Uchida, Phys. Rev. B 41 (1990) 865.
[20] D.C. Mattis, J. Bardeen, Phys. Rev. 111 (1958) 412.
[21] L.H. Palmer, M. Tinkham, Phys. Rev. 165 (1968) 588.
[22] G.A. Thomas, J. Orenstein, D.H. Rapkine, M. Capizzi, A.J. Millis, R.N. Bhatt, L.F. Schneemeyer, J.V. Waszczak, Phys. Rev. Lett. 61 (1988) 1313.

[23] T. Timusk, D.B. Tanner, in: D.M. Ginsberg (Ed.), Physical Properties of High Temperature Superconductors I, World Scientific, Singapore, 1989, p. 339.
[24] D.B. Tanner, T. Timusk, in: D.M. Ginsberg (Ed.), Physical Properties of High Temperature Superconductors III, World Scientific, Singapore, 1992, p. 363.
[25] For a review, see D.C. Johnston, F. Borsa, J.H. Cho, F.C. Chou, L.L. Miller, D.R. Torgeson, D. Vaknin, J. Zarestky, J. Ziolo, J.D. Jorgensen, P.G. Radaelli, A.J. Shultz, J.L. Wagner, S.-W. Cheong, W.R. Bayless, J.E. Schirber, Z. Fisk, in: E. Sigmund, K.A. Müller (Eds.), Phase Separation in Cuprate Superconductors, Springer, Berlin, 1994, p. 82.
[26] C.M. Varma, P.B. Littlewood, S. Schmitt-Rink, E. Abrahams, A.E. Ruckenstein, Phys. Rev. Lett. 63 (1989) 1996.
[27] A. Virosztek, J. Ruvalds, Phys. Rev. B 42 (1990) 4064.
[28] A. Virosztek, J. Ruvalds, Physica B 165 & 166 (1990) 1267.
[29] P.J. Hirschfeld, W.O. Puttika, P. Wölfle, Phys. Rev. Lett. 69 (1992) 1447.
[30] S. Quinlan, P.J. Hirschfeld, D.J. Scalapino, Phys. Rev. B 53 (1996) 8775.
[31] S.L. Cooper, A.L. Kotz, M.A. Karlow, M.V. Klein, W.C. Lee, J. Giapintzakis, D.M. Ginsberg, Phys. Rev. B 45 (1992) 2549.
[32] D.B. Romero, C.D. Porter, D.B. Tanner, L. Forro, D. Mandrus, L. Mihaly, G.L. Carr, G.P. Williams, Solid State Commun. 82 (1992) 183.
[33] M.A. Quijada, D.B. Tanner, F.C. Chou, D.C. Johnston, S-W. Cheong, Phys. Rev. B 52 (1995) 15485.
[34] T. Holstein, Phys. Rev. 96 (1954) 535.
[35] T. Holstein, Ann. Phys. 29 (1964) 410.
[36] J. Orenstein, S. Schmitt-Rink, A.E. Ruckenstein, H. Kuzmany, M. Mehrig, J. Fink (Eds.), Electronic Properties of High-T_c Superconductors and Related Compounds, Springer Series in Solid State Sciences, vol. 99, Springer, Berlin, 1990.
[37] P.B. Littlewood, C.M. Varma, J. Appl. Phys. 69 (1991) 4979.
[38] D.B. Romero, C.D. Porter, D.B. Tanner, L. Forro, D. Mandrus, L. Mihaly, G.L. Carr, G.P. Williams, Phys. Rev. Lett. 68 (1992) 1590.